Lag Relationships Involving Tropical Sea Surface Temperatures

JOHN R. LANZANTE

Geophysical Fluid Dynamics Laboratory/NOAA, Princeton University, Princeton, New Jersey

ABSTRACT

A long historical record (~100 years) of monthly sea surface temperature anomalies from the Comprehensive Ocean–Atmosphere Data Set was used to examine the lag relationships between different locations in the global Tropics. Application of complex principal component (CPC) analysis revealed that the leading mode captures ENSO-related quasi-cyclical warming and cooling in the tropical Pacific Ocean. The dominant features of this mode indicate that SST anomalies in the eastern Pacific lead those of the central Pacific. However, a somewhat weaker aspect of this mode also indicates that SST anomalies in the tropical Indian and western tropical North Atlantic Oceans vary roughly in concert with each other but lag behind those in the central and eastern Pacific. The stability of these lag relationships is indicated by the fact that the leading mode is quite similar in three different 30-year time periods.

In order to further examine these relationships some simple indexes were formed as the average over several grid points in each of the four key areas suggested by the CPC analyses. Several different types of analyses including lag correlation, checking the correspondence between extrema, and visual examination of time series plots were used to confirm the relationships implied by the CPC spatial patterns. By aggregating the lag correlations over the three 30-year time periods and performing a Monte Carlo simulation the relationships were found to be statistically significant at the 1% level. Reasonable agreement in the pattern of lag correlations was found using a different SST dataset.

Without aggregation of the lag correlations (i.e., considering each 30-year period separately) the areas in the Pacific and Indian were consistently well related, but those involving the North Atlantic were more variable. The weaker correlations involving the Atlantic Ocean underscore the more tenuous nature of this remote relationship. While major ENSO-related swings in tropical Pacific SST are often followed by like variations in a portion of the Atlantic, there are times when there is either no obvious association or one of opposite sign. It may be that while ENSO variability tends to have an impact in the Atlantic, more localized factors can override this tendency. This may explain some of the contradictory statements found in the literature regarding such remote associations.

In comparing the findings of this project with some studies that utilize very recent data (since about 1982) some discrepancies were noted. In particular, some studies have reported evidence of 1) an inverse relationship between SST anomalies in the tropical Pacific and those in the eastern tropical South Atlantic and 2) the appearance of ENSO-related SST anomalies in the central tropical Pacific prior to those in the eastern tropical Pacific. From a historical perspective both of these characteristics are unusual. Thus, the recent time period may merit special attention. However, it is important to stress that caution should be exercised in generalizing findings based only on this recent time period.

1. Introduction

The El Niño–Southern Oscillation phenomenon is generally acknowledged to be the largest component of the interannual variability of the global coupled atmosphere–ocean system. As pointed out recently by Latif and Barnett (1995), most related air–sea interaction studies have focused on the tropical Pacific where the ENSO signature is the strongest. They recently performed a series of modeling experiments based on both general circulation models and statistical models. The first canonical correlation mode (relating global SST

to zonal wind stress) from one of their experiments, based on the period from 1979 to 1988, indicated that during warm (cold) events in the tropical Pacific the tropical Indian Ocean was anomalously warm (cold) while the tropical Atlantic was anomalously cold (warm). They concluded that air–sea interactions in further integrations for time periods from 1979 to 1992 were consistent with this canonical mode. However, they also noted a discrepancy between their findings and those of Zebiak (1993), who concluded that SST in the equatorial Atlantic is uncorrelated with that in the tropical Pacific during the time period 1979–88.

In a somewhat similar type of analysis conducted by Lau and Nath (1994), a positive correlation was found between observed tropical SST anomalies in the Pacific, Indian, and Atlantic Oceans based on the first mode of singular value decomposition (SVD) involv-

Corresponding author address: Dr. John R. Lanzante, U.S. Department of Commerce/NOAA, Geophysical Fluid Dynamics Laboratory, Princeton University, P.O. Box 308, Princeton, NJ 08542.

ing global SST and Northern Hemisphere 500-mb height for the time period 1946–88. Similar relationships were found when an atmospheric GCM was forced with observed SSTs for the same time period.

In commenting on remote relationships in the Tropics Philander (1990) stated that much of the tropical Atlantic interannual variability is independent of the Southern Oscillation. He cited as exceptions the 1982–83 (1984–85) warm (cold) event in the Pacific, which was cold (warm) in the Atlantic. Similarly, Tourre and White (1995) found tropical Pacific and tropical Atlantic SST anomalies out of phase during most of the period from 1979 to 1991. By contrast, the first empirical orthogonal function of global SST for the time period 1949–79 derived by Hsiung and Newell (1983) as well as the first rotated EOF for the time period 1955–88 derived by Kawamura (1994) indicate that SST in the tropical Indian and Atlantic are positively correlated with tropical Pacific SST. Essentially, the same type of pattern was arrived at by Pan and Oort (1990) by applying correlation analysis over the time period 1870–1979; related lag correlations indicated a slight lead (1–3 months) of the tropical Pacific relative to the tropical Indian and Atlantic Oceans. Covey and Hastenrath (1978) composited SSTs from ten warm and ten cold events from 1911 to 1972; these composite maps showed mixed positive and negative anomalies in the tropical Atlantic with perhaps more of the same sign as in the tropical Pacific.

While the studies cited above generally indicate that tropical Pacific SST anomalies are typically accompanied by anomalies of like sign in the tropical Indian Ocean, they present a seemingly contradictory or confused picture of the relationship with SST in the tropical Atlantic. This paper reports an investigation of the *lagged* interrelationships of SST in the global Tropics and attempts to clarify the above picture and suggest reasons for the *apparent* discrepancies. The purpose is to establish that such lag relationships exist and are reproducible in a long historical record. The intent is not so much to determine precise lags between different regions but rather the sequence (order) in which anomalies appear. The nature of the tropical SST field may be of relevance to the diagnosis and prediction of short-term climate variability given that some degree of success in simulating the global atmospheric circulation has been attained in forcing atmospheric general circulation models with observed tropical SST anomalies (Lau and Nath 1994; Graham et al. 1994).

The outline of this paper is as follows. The data and preparation, including the filtering used, are described in section 2. The nature of the lag relationships and their reproducibility in subsamples of the record are given in section 3 based on complex principal component (CPC) analysis. Lag correlation analysis is performed in section 4 using indices motivated by the CPC patterns in order to confirm the relationships uncovered by the CPC analysis and assess significance; reproduc-

ibility in subperiods as well as in another SST dataset is also addressed. Section 5 examines the correspondence between the main features (extrema) of the index time series both objectively (§5a) and subjectively through visual examination (§5b). Finally, a discussion of the results, including interpretation and some speculation, concludes this paper (§6).

2. Data and preparation

The primary data used (Woodruff et al. 1987) are the SSTs from the Comprehensive Ocean–Atmosphere Data Set (COADS), which were available on a monthly basis in the form of 2° latitude × 2° longitude boxes. Objective analysis (Pan and Oort 1990) was used at the Geophysical Fluid Dynamics Laboratory (GFDL) to place these data on a 1° latitude × 1° longitude grid for the time period 1870–1988. In this study 315 grid points (a subset of the GFDL analysis) on a staggered 5° latitude × 5° longitude grid were used; the locations can be inferred in subsequent figures as the center of the plotted vectors.

The GFDL analysis scheme blends the gridbox data and may be expected to have an effect similar to spatial averaging or spatial smoothing. In addition, any missing values are filled by this spatial interpolation scheme. In order to insure that the lead–lag relationships sought were not being distorted by this, or in fact any other characteristic related to the COADS processing, some of the calculations were repeated using SSTs from the Global Ocean Surface Temperature Atlas (GOSTA) compiled by Bottomley et al. (1990). These data are available on a 5° latitude × 5° longitude grid and do have monthly values reported as missing when insufficient observations were available.

The statistical analyses performed in this work were done separately for each of three different 30-year periods: 1) 1875–1904, 2) 1910–39, and 3) 1950–79. Some of the analyses were then aggregated over these three periods. There are several reasons for this approach. Figure 9 of Pan and Oort (1990) indicates that there is considerable interdecadal variability in SST averaged over the Tropics and over the globe. In particular, there is a noticeable drop during the first decade of the twentieth century and a rapid rise near 1940 (which may be due in large part to the change from bucket to ship intake SST measurements). Use of the three time periods eliminates most of the influence of these step function–like changes, which are not of interest here. Some of the data deficient period associated with the Second World War is also removed in this scheme; however, the middle period is degraded by virtue of the effects of the two World Wars. In addition, the use of several independent time periods allows for an assessment of the reproducibility of the results, particularly in light of the varying quality and spatial coverage of the data over the historical record. Choice of a 30-year interval, while arbitrary, has some prece-

dence in that it is favored for use in calculating climatological normals. Also, any 30-year period is likely to encompass several ENSO-related warm and cold events, which tend to dominate the variability of the Tropics.

The data used in much of the analyses reported here (sections 3 and 4) have been lightly low-pass filtered using a Lanczos filter (Duchon 1979) with weights extending out ±6 months and a cutoff frequency corresponding to a period of 4 months. This removes very high frequency noise, which is not relevant here; with regard to CPC analysis, which is discussed below, such noise could distort the complex representation of the data (Horel 1984). For some of the analyses in which more strongly low-pass filtered data were needed, similar filters with cutoffs corresponding to 15 months (section 5b) and 18 months (section 5a) were also employed. The former has weights that extend out ±30 months, while the latter, which provides a sharper cutoff, extends out ±60 months.

3. Complex principal component analysis

The analyses performed here utilized both sophisticated and simple techniques, the former for their power to explore complicated relationships and the latter in a confirmatory and explanatory fashion. CPC analysis was used to identify the key areas involved in the lag relationships. A tutorial on the use of this technique is given by Horel (1984). Like its real counterpart, CPC analysis is able to organize the complicated interrelationships in a multivariate dataset into a relatively few modes of variability. However, analysis in the complex domain allows for the depiction of lag relationships, which are not explicitly resolved by real PC analysis. As pointed out by Barnett (1983), CPC analysis operates in the time domain and is better suited for the analysis of episodic, cyclo-stationary, quasi-periodic phenomena, such as ENSO variability, than other common techniques, such as cross-spectral analysis.

The CPC analyses were carried out by first applying the light low-pass filter (as described in section 2) to each gridpoint time series in order to form the real part of the complex data. Next a fast Fourier transform was applied to the filtered data. The imaginary part was formed by transposing and/or negating the sine and cosine coefficients at each frequency to produce a quadrature time series (Horel 1984). The resulting complex time series were used to calculate the complex correlation matrix, which is Hermitian. The eigenvalue solution of this matrix yields real eigenvalues and complex eigenvectors.

In the application of CPC analysis rotation using the varimax criterion was also used (Horel 1984). This rotation had virtually no effect on the first modes (for each 30-year period), which each explains ~20% of the variance. After the first mode the eigenvalues drop precipitously, and both the spatial patterns (eigenvec-

tors) and time series lack the appearance of physically realistic modes. These higher order modes were considered noise and were not retained for interpretation. This result is not surprising in so much as the first mode captures ENSO-related variability, which tends to dominate in the Tropics.

For the purposes of presentation, the complex eigenvectors are plotted on maps in vector form; this allows for the simultaneous representation of both amplitude and *relative* phase information. In these maps a vector is plotted (centered at each grid point) such that its length is proportional to the amplitude and its angle indicates relative phase. In this representation vectors that point in opposite directions indicate an out of phase relationship, those at right angles are in quadrature, etc. Because of the conventions adopted here, propagation is indicated by a counterclockwise rotation of nearby vectors. A large vector located in the lower right-hand corner of each map is a reference vector; its magnitude is 1, the maximum possible value, indicating a perfect correlation. For easier comparison the phases (angles) of the vectors have been oriented so that the vector on the equator at the date line points up.

The complex eigenvectors corresponding to the first mode for each of the 30-year periods are shown in Figs. 1a–c, and their explained variances (%) are: 20.2 (1875–1904), 16.3 (1910–1939) and 21.5 (1950–1979). The somewhat lower value during the middle period could be a reflection of data degradation (sparsity) associated with the World Wars, although there are some suggestions that the amplitude of tropical warmings and coolings was reduced during this time period (Rasmusson and Carpenter 1982; Gu and Philander 1995). Inspection of the three eigenvectors indicates considerable similarity for this mode, which depicts ENSO-related tropical warming and cooling. Given the changes in data quality and quantity over the historical period this similarity is remarkable and attests to the robustness of the basic SST-related features associated with ENSO variability in the climate system.

This mode of SST variability is characterized by large amplitude throughout most of the Tropics between 20°N and 20°S. Closer examination indicates several important lag relationships. The well-established westward migration of anomalies from the waters off the west coast of South America to the central Pacific is depicted by the counterclockwise rotation of the vectors between these two regions. Note also two regions of relatively large amplitude and coherent phase located in the Indian and North Atlantic Oceans. The vectors in these two regions have a counterclockwise angular displacement relative to the region at the equator near the date line, indicating a further lag. Note that these relationships do not necessarily imply that water or heat is advected or transported from one region to the next; rather they indicate the sequence in which anomalies appear. In summary, anomalies of one sign first appear off the west coast of South America, then

in the central Pacific, and later in the Indian and North Atlantic Oceans.

There are also some areas that do not appear to play a consistent part in this mode: for example, most of the areas poleward of 20° latitude in the Pacific and Indian Oceans, the South Atlantic, and in the vicinity of the region north of New Guinea. In these areas the vector arrows are either not consistently large and/or have different orientations between the 30-year periods. However, with regard to these inconsistencies it should be kept in mind that the data quality and spatial coverage vary considerably over the time period examined here. Pan and Oort (1990) present maps that depict the spatial density of observations for each decade from 1870 to 1979. The interested reader is invited to compare those maps with the eigenvectors shown in Fig. 1. Generally speaking, for the last 30-year period used here (1950–79) the data coverage is reasonable throughout the Tropics with spotty gaps in only limited areas. During the earlier periods data coverage in the tropical Indian and Atlantic Oceans is characterized to some extent by gaps and tends to improve gradually

with time. However, in the earlier periods the coverage in the tropical Pacific is sparse, except for the eastern third and the extreme western portions adjacent to coastal regions of Southeast Asia, Indonesia, Australia, and New Zealand. In addition, an apparent shipping route provides data during most of the historical record running approximately from eastern Australia to Fiji to British Columbia, transecting the important region near the equator and date line. While the Pacific coverage does improve from the first to the second 30-year period, it is not until 1930–39 that the large data void begins to fill significantly. In summary, results for the final 30-year period are considered more reliable. The inconsistencies noted above tend to fall in the regions of poorer coverage during the earlier years; therefore, it may not be wise to attach much significance to these inconsistencies. In spite of these data concerns, the major aspects are well reproduced during all three periods. One possible reason for this is the dominance of ENSO-related variability in the Tropics. Another reason is that the impact of spatial and temporal gaps in the data is diminished by the fact that these ENSO-related varia-
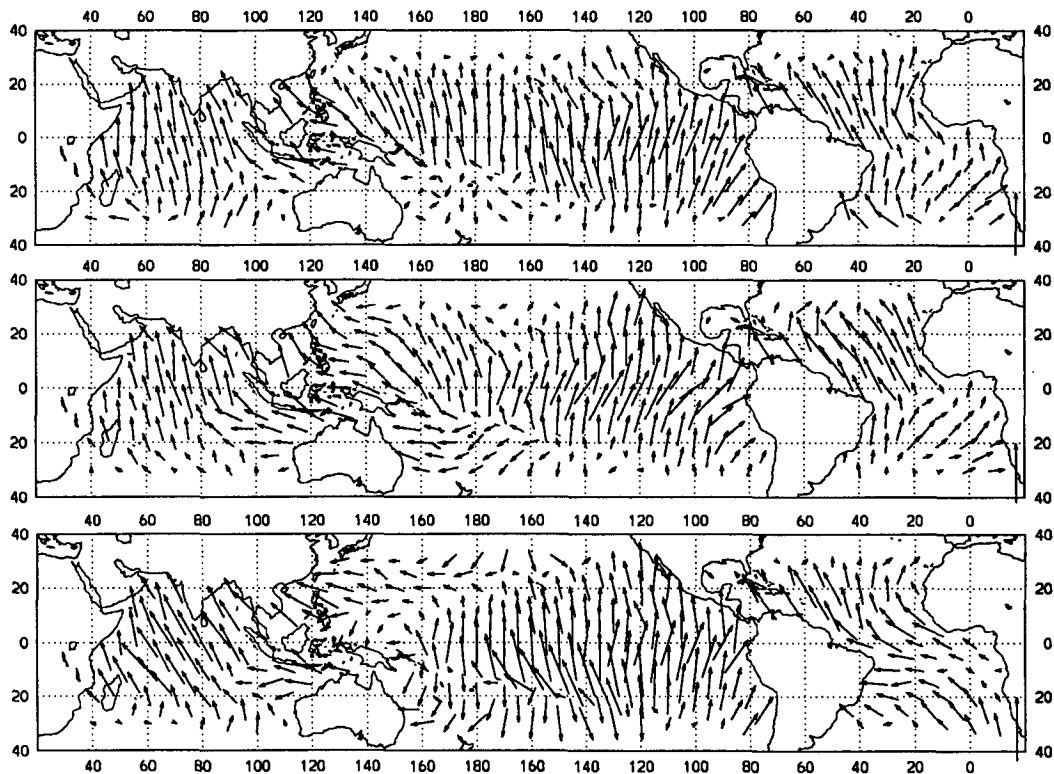

FIG. 1. First complex eigenvector from CPC analysis of 30 years of COADS SST for the periods (a) 1875–1904 (top), (b) 1910–1939 (middle), and (c) 1950–1979 (bottom), which explain 20.2%, 16.3%, and 21.5% of the variance, respectively. A vector is plotted at each grid point such that its length is proportional to the magnitude and its orientation (angle) is proportional to the relative phase. The reference vector plotted in the extreme lower right corner of each panel has unit magnitude, which is the largest possible value. Vectors that are oriented in the same direction indicate a perfectly in-phase relationship, while those that point in opposite directions are perfectly out of phase, etc. For consistency among the three panels the vectors have been adjusted so that the vector at the equator on the date line points up. Propagation occurs in the direction in which the vectors rotate counterclockwise.

tions tend to occur on longer time and larger spatial scales.

It has been pointed out by N.-C. Lau (1995, personal communication) that the lags in phase between SST in different regions throughout the Tropics, depicted in Fig. 1, are qualitatively consistent with cross-spectral analyses based on the ensemble of four Global Ocean–Global Atmosphere GCM experiments, which were diagnosed by Lau and Nath (1994). More specifically, the cross-spectrum at ~2–4 year periods indicates that SST averaged over a portion of the eastern and central tropical Pacific leads SST in portions of the tropical Indian and western tropical North Atlantic by ~1/4 cycle.

It should be kept in mind that the relative lags depicted by the eigenvectors (Fig. 1) in terms of an angular difference imply lags expressed in units of a fraction of a cycle. Since the ENSO cycle varies in period, these lags do not necessarily imply a fixed interval of time. However, while El Niño episodes generally occur every 2–7 years, what is most relevant to this matter is the rate at which the cycle proceeds when an event (warm or cold) is in progress. The biennial timescale, which has been documented by Rasmusson et al. (1990), seems applicable here. For example, looking at Figs. 10 and 11 of Rasmusson and Carpenter (1982), it is apparent that the typical time from zero anomaly to peak warm or cold and back to zero is ~1 year. This suggests that the angular lags in Fig. 1 should correspond to a typical lag of about 3 months (phase difference ~ 1/8 cycle) between the eastern and central Pacific and about 6 months (~1/4 cycle) between the eastern Pacific and the Indian and North Atlantic regions; this is verified later.

The correspondence of the leading eigenvector to ENSO-related tropical SST variability has been further confirmed through the use of a sequence of composite maps (not shown) generated from the complex (principal component) time series associated with mode 1. The CPC phase function was arbitrarily partitioned into eight nonoverlapping bins of equal angular width ($2\pi/8$). Each observed monthly SST map was placed into its appropriate bin, and then all of the maps in each bin were averaged. This sequence of maps depicts one complete typical cycle. The evolution of anomalies over such sequences of maps was found to correspond well with the accepted ENSO-related SST cycle.

Another way of validating the CPC representation is through a comparison of the CPC time series with those from gridpoint locations or area averages. An example of this type of comparison for the 1950–79 period is shown in Fig. 2. The top curve is an index that represents the average SST over the five grid points from the central Pacific, denoted as CPAC in Fig. 3. For convenience this index has been standardized to have zero mean and unit variance. A visual comparison with indices reported by Wright (1989) gives the impression that the major warm and cold events are fairly well represented by this simple index.
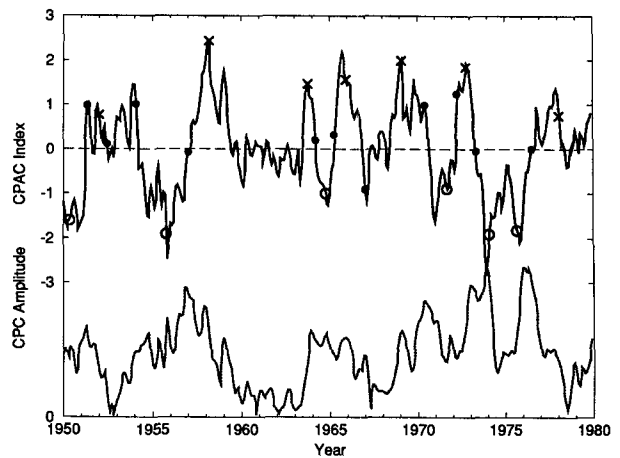

FIG. 2. Time series of CPAC index (top, solid) and CPC amplitude (bottom, dotted) for the period 1950–79. The CPAC index has been computed by averaging the SST anomalies over the grid points shown in Fig. 3, followed by a standardization to zero mean and unit variance. The CPC amplitude (arbitrary units) is the magnitude of the complex time series corresponding to the eigenvector in Fig. 1c. Certain phases from the phase function corresponding to the time series of the CPC eigenvector of Fig. 1c have been superimposed as the symbols on the CPAC time series. The estimated times of peak warming (X) and cooling (O) are indicated along with the inflection points (dots). No phase symbols can be plotted when the CPC amplitude is small because the phase becomes noisy since the mode is irrelevant at this time.

The CPC amplitude time series (a nonnegative quantity), which measures the strength of the mode, is plotted as the lower (dotted) curve in Fig. 2; it is scaled in arbitrary units. The amplitude is large when warm and cold ENSO *cycling* is pronounced. For example, from about 1954–58 the CPC amplitude is large, during which time a large amplitude oscillation from cold to warm is observed. Note that because the CPC amplitude is based on lag information and is a measure of the strength of *oscillation*, it may be large when the SST anomaly is near zero (for example, during early 1957). Another prominent period of large amplitude occurs over most of the time period from the early 1960s to late 1970s, during which time several prominent oscillations occurred. By contrast there are times when the amplitude is small and the tendency for cyclical behavior is absent, such as during 1960–63.

A companion to the CPC amplitude time series is the CPC phase; together they completely represent the time behavior of a CPC mode. While the former indicates the strength of the oscillation, the latter indicates the (angular) position within the cycle. In the interest of simplicity, instead of plotting the phase function several key phase positions have been plotted and are represented by the symbols in Fig. 2. These points were determined by first averaging the phase of the eigenvector (Fig. 1c) over the five CPAC grid points (Fig. 3) to determine the approximate phase that corresponds to the center of a warm peak in this area; the cold trough
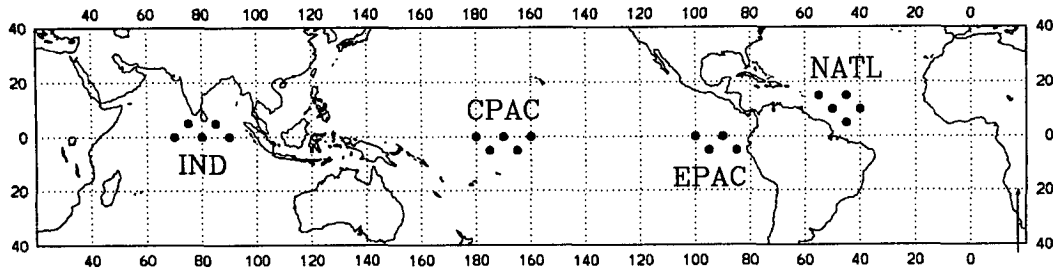
FIG. 3. Locations of COADS grid points used for the construction of the SST indexes in the Indian (IND), central Pacific (CPAC), eastern Pacific (EPAC), and North Atlantic (NATL) Oceans.

is centered at a displacement of π and the inflection points (rising or falling) lie in between. Next, proceeding sequentially through the CPC phase time series, each time point having a corresponding phase closest to each of these four key phase values was denoted by a symbol in Fig. 2 (X: warm, O: cold, and dot: inflection). The phase tends to vary quasi-linearly except during time periods when the amplitude is very small; no key points were plotted during these times.

Looking at the symbols in Fig. 2 it appears that there is a reasonably good correspondence between the behavior of the CPAC index and the key features of the CPC phase function. Note that this comparison involving the phase, as well as the earlier ones involving the amplitude, is a quite severe test. This is true because, while the SST index measures the behavior over a very small area, the CPC time series captures the lag behavior over a large portion of the Tropics. Nevertheless, the veracity of the CPC representation as well as the large-scale coherence of the ENSO phenomenon are in evidence.

4. Lag correlations

CPC analysis is a very powerful multivariate technique that has been shown to capture the essential ENSO-related SST variability in the Tropics. As applied here, it has indicated several lag relationships that are reproducible in separate portions of a long historical record of SST data. At this point it is desirable to examine the strength and reproducibility of these lag associations using a simpler, more traditional approach, namely, lag correlation analysis. Since this and other techniques similar in nature are more widely used, the degree of reproducibility may offer some insight as to reasons for some of the contradictions in the literature cited earlier. It is proposed that the power of the CPC technique enhances the detection of some of the weaker aspects of the lag relationships that are more easily obscured when using this simpler approach. Nevertheless, it will be demonstrated that even using this simpler approach the lag associations can be shown to be highly statistically significant when viewed from the context of a long historical record. Furthermore, lag correla-

tions are useful in refining quantitative estimates of the lag times.

In order to facilitate the lag correlation analyses several indexes have been derived by averaging the SST anomaly over four or five grid points; the locations are shown in Fig. 3. The areas/points were chosen subjectively from the examination of the complex eigenvectors (Fig. 1) and represent indexes of the key areas involving lag relationships, which were discussed earlier. These areas include the waters near the coast of South America (EPAC) where the warming/cooling is first in evidence, the central Pacific (CPAC) where the changes occur next, and the more remote areas in the Indian (IND) and North Atlantic (NATL), which lag still further.

Lag correlations were computed between each of the six possible combinations of indexes for lags ranging out to ±12 months. For each, the correlation having the largest magnitude and its corresponding lag are given in Table 1, separately for each 30-year period and (bottom) as the average of the three separate correlation functions; the average correlations were arrived at by first applying Fisher's z transformation, averaging the transformed values, and then inverse transforming the averages (Zar 1974). Because of the considerable persistence in the observed indexes and corresponding reduction in effective degrees of freedom, direct application of standard correlation critical values is inappropriate. Instead, the significance level (α) was approximated using 2000 trials in Monte Carlo simulations in which the observed time series were replaced by random series, which are first-order autoregressive; the estimated lag-1 (month) autocorrelations (which are typically ~0.90–0.95) from the observed indexes for the time period 1950–79 were used. This constitutes a conservative approach in that (i) the 1950–79 lag-1 autocorrelations are slightly larger than for other time periods and (ii) while a second-order autoregressive process may have produced a better fit in one case (EPAC), it would tend to make it easier to attain significance since the persistence time would be reduced.

The COADS correlations in Table 1 confirm the conclusions drawn earlier based on the CPC analyses. While most of the 30-year correlations are at least sig-

TABLE 1. Largest magnitude correlations (*r*) between the indexes, as defined in Fig. 3, according to lag (months) in the range of ±12 months. For positive lag, index 1 leads index 2. Correlations are for a 30-year period or (bottom) the average over the three 30-year periods and are based on either COADS or GOSTA SST data. For GOSTA, when too few values were available no correlation was computed; a "?" indicates that only about half of the months were available for correlation. Significance level (COADS only) is based on a Monte Carlo simulation. Correlations in italics are significant at the 5% level, those in bold are significant at the 1% level.

Years	Index 1	Index 2	COADS		GOSTA	
			Lag	*r*	Lag	*r*
1875 to 1904	EPAC	CPAC	0	**0.56**	—	—
	EPAC	IND	6	**0.46**	—	—
	EPAC	NATL	7	**0.44**	—	—
	CPAC	IND	1	**0.50**	—	—
	CPAC	NATL	3	*0.41*	—	—
	IND	NATL	−1	**0.53**	−1	0.48
1910 to 1939	EPAC	CPAC	4	**0.48**	4	0.23?
	EPAC	IND	6	*0.37*	7	0.48?
	EPAC	NATL	5	0.24	3	0.23?
	CPAC	IND	3	**0.42**	3	0.39?
	CPAC	NATL	4	0.15	5	0.14?
	IND	NATL	0	*0.41*	0	0.41
1950 to 1979	EPAC	CPAC	3	**0.65**	3	0.71
	EPAC	IND	5	*0.44*	4	0.45
	EPAC	NATL	6	0.34	6	0.29
	CPAC	IND	2	**0.66**	2	0.59
	CPAC	NATL	4	*0.51*	5	0.43
	IND	NATL	1	0.41	1	0.09
Average	EPAC	CPAC	4	**0.55**	—	—
	EPAC	IND	6	**0.42**	—	—
	EPAC	NATL	7	**0.33**	—	—
	CPAC	IND	2	**0.53**	—	—
	CPAC	NATL	4	**0.36**	—	—
	IND	NATL	0	**0.45**	—	—

nificant at the 5% level, confidence is increased by aggregating over the three periods since all of the average correlations are significant at the 1% level. Both the magnitude and lag are fairly well reproduced in each period, although the middle time period produces the weakest correlations in all cases, especially those between the Atlantic and Pacific indexes. The picture that emerges is that of the appearance of anomalies first in the eastern Pacific, followed by the central Pacific about 4 months later, and then the Indian and Atlantic Oceans a couple of months later.

As discussed in section 2, it is desirable to determine to what extent the fundamental lag relationships are influenced by the preparation of the data. As such, the COADS lag correlation analyses have been repeated using the GOSTA SST data. Since the grids are offset slightly from one another, the locations used for the GOSTA indexes differ slightly from those shown in Fig. 3. As previously noted, the GFDL COADS spatial analysis scheme should have the effect of a mild spatial smoothing or averaging; thus the GOSTA indexes are slightly noisier than their COADS counterparts. Also, the GFDL scheme uses spatial interpolation so that there are no missing values. As a result of missing values there were too few observations for GOSTA cor-

relation analyses for most of the early period. During the middle period only about half of the observations were present, so these are presented in a more cautionary manner and are denoted by a "?" in Table 1. With only a few exceptions the GOSTA and COADS correlations shown in Table 1 correspond rather well in terms of both the correlation and the lag. Overall, it seems as if the essential relationships are not very specific to the manner in which the data were prepared.

5. Correspondence between indexes

In the two prior sections the nature of the lead/lag relationships involving tropical SSTs have been characterized in terms of summary statistics. The complex correlations that constitute the CPC eigenvector pattern represent the relationships in a sophisticated fashion, while the lag correlations of the indexes provide such characterization using a more traditional approach. While such summary statistics are very useful, it is also desirable to examine the variability in the lags from case to case. This issue is addressed in two different ways in this section. In section 5a a frequency distribution of the lags between extrema in the time series in each pair of the indexes is given. In section 5b the

time series of the indexes are presented for the entire period of record. Together these analyses help to fill in the picture of the lag relationships more completely.

a. Distribution of lags between extrema

The nature of the lag relationships between the different key regions (identified previously) are explored here via frequency distributions. These frequency distributions represent the number of occurrences that a maximum (minimum) of one index was associated with a maximum (minimum) in another index for a given lag between indexes. The extrema were required to have a relative maximum (minimum) for a positive (negative) anomaly. However, in order to avoid generating a large number of small amplitude extrema it was necessary to apply a stronger low-pass filter, having a cutoff frequency corresponding to a period of 18 months. Additionally it was required that maxima (minima) be separated by more than 18 months; when extrema were too close, the one(s) having smaller magnitude were eliminated. These constraints helped ensure that each "event" was characterized by a single extremum and resulted in values that looked reasonable based on visual inspection. It should be kept in mind that by virtue of the filtering emphasis is placed on the lower frequency variations so that some temporal resolution is sacrificed. The frequency distributions render a somewhat smoothed representation of the lag/lead relationships. It is the general nature of the frequency distribution and their correspondence to previous analyses that are of most interest here.

The lag frequency distributions just described are given in Table 2. These values are aggregates of separate analyses for each of the three 30-year time periods used in prior analyses, thus making the statistics from the average in Table 1 directly comparable with Table 2. For each combination of indexes the frequency of co-occurrence of extrema is given for a range of lags. For example, given an extremum in EPAC, a similar extremum is found in CPAC 1–3 months later 35% of

the time. By comparison of Tables 1 and 2 it can be seen that the lag of maximum correlation (average) from Table 1 corresponds well with the region of maximum histogram density in Table 2; also, the stronger correlations have a larger concentration of density. The associations involving the Pacific and Indian indexes are more concentrated than those involving the Atlantic. In particular, the relationship between IND and NATL is more diffuse and, in contrast to the correlations, suggests more of a tendency for NATL to lead IND.

The nature of these distributions also explains some of the results from the earlier analyses. With regard to the reproducibility between the three 30-year periods, the CPC analysis seemed somewhat less variable for the more remote associations involving the Indian and especially the North Atlantic regions than did the lag correlations. The more diffuse nature of the corresponding histograms of Table 2 suggests more variability in the lag time. The CPC analysis performs better since it is able to explicitly incorporate this aspect, whereas the lag correlations are subject to "smearing."

b. Time series

Perhaps the simplest way to characterize the lag relationships involving tropical SST is by examination of the time series. For this purpose the entire ~120-year series corresponding to each of the indexes in Fig. 3 has been filtered using a 15-month low-pass filter. The low-pass filter used here is not as sharp as the one used in section 5a and, therefore, results in the loss of less data from the ends of the series; visual inspection does not require as much sharpness as the determination of extrema in the previous section. Each time series has also been detrended; this was not a concern earlier because the 30-year periods were chosen to largely avoid this issue. After filtering and detrending, all available data in each of three ~40-year periods (1872–1909, 1910–1949, and 1950–1986) were standardized separately to produce series with zero mean and unit vari-

TABLE 2. Frequency distributions of co-occurrences of extrema by lag (months). The indexes are as defined in Fig. 3. Data from 1875–1904, 1910–1939, and 1950–1979 were used. For positive (negative) lag the value in each cell is the percentage of the time that an extremum in index 1 is followed (preceded) by an extremum of the same type for index 2, within the given lag range. The last column is the sum of all of the occurrences from lags −12 to +12; the sum of the cells does not always equal this value due to rounding of cells to the nearest integer value. An 18-month low-pass filter was applied to the time series involved and extrema of the same type were required to be more than 18 months apart; when closer extrema were found, those of smaller magnitude were eliminated.

Index 1	Index 2	−12/−10	−9/−7	−6/−4	−3/−1	0	1/3	4/7	7/9	10/12	Sum
EPAC	CPAC	3	0	2	3	5	35	25	6	3	82
EPAC	IND	5	2	0	2	2	8	29	25	11	82
EPAC	NATL	5	3	0	6	2	12	14	14	11	66
CPAC	IND	0	2	2	5	5	44	19	2	3	81
CPAC	NATL	0	2	10	6	3	17	11	14	3	67
IND	NATL	3	8	12	14	5	8	8	5	5	69

ance. This preparation allows for easier visual assessment of the relationships of the phases and relative amplitudes of low frequency variations amongst the indexes. These time series are displayed in Figs. 4a–c.

Starting with the first time period (Fig. 4a), it can be seen that the spread of anomalies from the eastern Pacific to the central Pacific, and later to the Indian and North Atlantic, is generally apparent during major warm and cold events in the tropical Pacific. Particularly outside of the Pacific, the relationships are not as apparent when there is no major Pacific event. That the dominant lag relationships were contained in one mode associated with variability on ENSO timescales was indicative of this. In contrast to the typical sequence there are times when NATL appears to either lead slightly or be coincident with EPAC, such as during the warm event of 1896. During the warm event of 1888–89 and the cold event of 1892–95, due to double extrema the time series are ambiguous, but suggestive of a possible lead by NATL.

During the middle time period (Fig. 4b) the character of tropical Pacific variability appears to be somewhat different than in the earlier and later time periods. Specifically, the warm and cold spells are usually of shorter duration and are less coherent across the Tropics. Data degradation during the World Wars might explain some but not all of this change. Earlier it was seen that the dominant CPC mode explained somewhat less variance during this 1910–39 time period. The time series are somewhat suggestive of a greater dominance of a biennial timescale during this period. Nevertheless, the typical lag relationships are prominent in some of the major events of this time period.

During the final time period (Fig. 4c) the typical lag relationships can again be seen most clearly during the more significant events. Again, however there are times when the Atlantic and Indian do not follow the behavior of the Pacific as expected. For example, the cold periods in the Pacific during 1955–56 and 1962–63 are accompanied/followed by warm conditions in the Atlantic for the former and warm in both the Indian and Atlantic for the latter.

6. Discussion

The ENSO phenomenon is characterized by quasi-periodic warmings and coolings of the tropical Pacific Ocean, which in terms of SST anomalies first appear near the west coast of South America and later spread westward to the central Pacific. There has been much effort during the last decade or two to develop theoretical arguments in terms of coupled ocean–atmosphere dynamics to explain these occurrences. In this study a long record of historical observations of SST in the global Tropics has been used to reexamine the associated *evolution* of the SST anomaly field not only in the tropical Pacific but also in the Indian and Atlantic Oceans. Using several different approaches, it has been
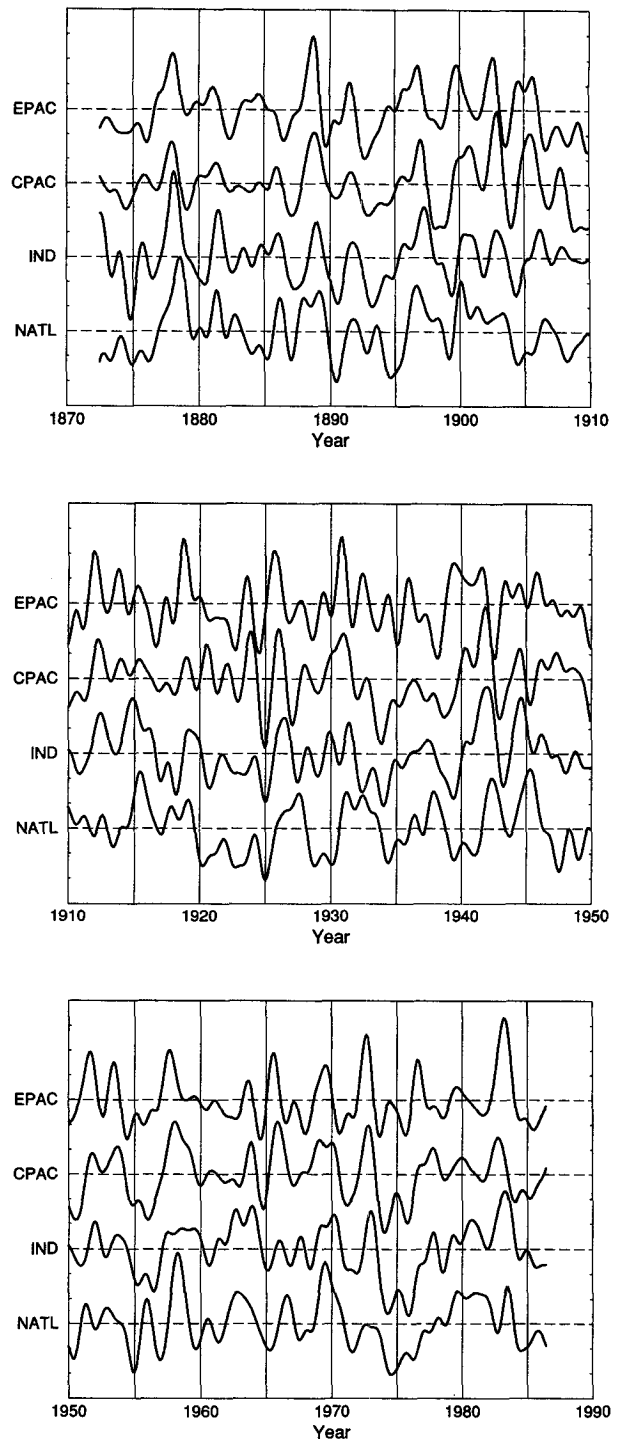

FIG. 4. Time series of the indexes from Fig. 3 covering the time period (a) 1872–1909, (b) 1910–1949, and (c) 1950–1986. A 15-month low-pass filter was applied to the original indices, which were then detrended; then each time series was standardized to zero mean and unit variance using just the data in the given time period. The filtering has resulted in the loss of 30 months of data from each end of the original series. Each dashed horizontal line is the zero axis for a particular index. Vertical tick spacing is one standardized unit.

shown that typically anomalies first appear in the eastern tropical Pacific, followed by the central Pacific ~3 months later, and then the Indian Ocean ~3 months after that. This sequencing of events is highly reproducible within different portions of the long historical record and by using different approaches. It should be noted, however, that the lag time between regions does vary somewhat from event to event.

A significant association of SST in a portion of the tropical western North Atlantic with SST variations in the tropical Pacific has also been established. The timing is such that the North Atlantic region lags behind the Pacific and is approximately coincident with variations in the Indian Ocean. The strength and subsample reproducibility of the lag associations involving the North Atlantic are somewhat weaker than those within the Pacific or between the Pacific and Indian Oceans.

As pointed out in section 1 there are a number of *seemingly* inconsistent statements in the literature regarding the association between events in the tropical Pacific and SST in the tropical Atlantic. It was seen here that confidence in the reality of the lag associations involving the western tropical North Atlantic is bolstered when utilizing the larger historical record, more so than for the other noteworthy associations; thus, atypical results may be reached when using smaller samples. Also, the North Atlantic associations show more variability in the time lag. This makes it more difficult when utilizing techniques such as lag correlation and composite analysis, which implicitly assume that the lag time does not vary from event to event. Finally, many studies only considered the contemporaneous association, which is weaker than in lag.

Several recent investigators have made statements that do not seem to agree with the conclusions of this study. Both Philander (1990) and Tourre and White (1995) noted an inverse relationship between tropical SST anomalies in the Atlantic and those in the Pacific during both the 1982–83 warm event and the subsequent 1984–85 cold event. Similarly, Latif and Barnett (1995) found a negative correlation between equatorial Pacific and Atlantic SST; however, Zebiak (1993) found a near-zero correlation for the same. The inverse relationship noted by Philander (1990), Tourre and White (1995), and Latif and Barnett (1995) reflects a contemporaneous SST association between the tropical Pacific and a region located in the eastern tropical Atlantic, mostly south of the equator, which was strongly evident during the 1982–83 warm event and the two subsequent cold events. Zebiak's Atlantic mode, while somewhat similar, has more emphasis farther west. Note that none of these areas share any appreciable overlap with the key area (NATL), which was identified in this study. The time periods in the cited studies are rather short compared to the periods of record used herein and, thus, can be dominated by this atypical inverse relationship, which dominated the 1980s. As seen in the CPC modes from Fig. 1, there is no evidence of

a particularly strong or consistent relationship in the region between 0° and 20°S in the Atlantic. Finally, the lag nature of the Pacific–Atlantic association may play a role. As can be seen in Fig. 4c, during much of the time that the Pacific (EPAC and CPAC) was warming during 1982–83, the North Atlantic (NATL) was slightly colder than normal; consistent with the relationship highlighted in this paper the North Atlantic lagged a number of months behind the Pacific.

Tourre and White (1995) also found evidence of weak *eastward* migration of SST anomalies in the tropical Pacific during the 1980s. This is inconsistent with the CPC analyses presented here (which do not extend beyond 1979). However, the time series shown in Fig. 4c appear to indicate this reversal, as evidenced by a slight lead of the central tropical Pacific SST anomalies (CPAC) over those in the eastern tropical Pacific (EPAC) during the early to middle 1980s. Thus, it is important to note that some of the behavior of tropical SST anomalies in recent years (since about 1982) is quite unusual from a historical perspective. For that reason this time period may be of special interest. Nevertheless, caution should be exercised in generalizing findings obtained using data from this atypical time period.

That changes in the Indian and North Atlantic regions lag behind those in the Pacific suggests that these regions are forced remotely from the Pacific. However, lag/lead relationships alone do not necessarily imply cause and effect. A plausible explanation given by Lau and Nath (1994), based on diagnosis of an atmospheric GCM forced by observed SST in the tropical Pacific from 1946 to 1988, is that ENSO activity in the Pacific teleconnects to more remote basins through an atmospheric bridge via anomalous fluxes. They found that SST anomalies in the tropical Indian and Atlantic Oceans were the result of anomalous heat fluxes induced by changes in the local atmospheric circulation, which themselves were instigated by a remote signal transmitted from the tropical Pacific through an "atmospheric bridge." Additionally, they found that in the western tropical North Atlantic (NATL region) the dominant factor during warm (cold) events was a reduction (increase) of wind speed resulting in reduced (increased) sensible and latent heat fluxes out of the ocean, while in the Indian (IND region) reduced (increased) cloudiness leads to an increase (decrease) in radiative flux into the ocean. In an observational study by Wolter (1987) cluster analysis was applied to sea level pressure (SLP), wind speed, cloudiness, and SST data in the Tropics for the period 1948–83. In relation to the Southern Oscillation, fluctuations of SST anomalies were seen to be global in nature, including the Indian and North Atlantic associations found here. Furthermore, some degree of consistency was found between the observational analysis of Wolter (1987) and the modeling studies of Lau and Nath (1994). Wolter's (1987) correlations are such that for tropical Pacific

warm (cold) events there is a strong indication of reduced (increased) wind speed in the North Atlantic during boreal winter and a strong indication of reduced (increased) cloudiness in the Indian during boreal summer.

Since the ENSO phenomenon can be understood in terms of ocean dynamics and air–sea coupling in the tropical Pacific and can be reproduced by models limited to that area, it seems reasonable to assume that the *essential* physics involves just the tropical Pacific; however, an interesting question is whether or not other areas play a role in modulating or perhaps *occasionally* aiding the initiation of Pacific events. Even if this is so, it may be that the mechanism described in the previous paragraph explains the major part of the *remote* lag relationships. It was noted in section 5 that occasionally SST changes in the Atlantic appear to lead those in the tropical Pacific. However, if the forcing does sometimes occur in the opposite direction from the typical relations found here, it would be very difficult using only the SST fields to demonstrate this convincingly — even using ~120 years of data. Given the small number of cases the reversals could be merely coincidental. At least a very careful diagnostic analysis of the relevant forcing terms estimated from observed data would be necessary, and given concerns about data quantity and quality in the relevant areas, model simulations in which the SST anomalies were either prescribed as observed or withheld for different combinations of the key areas would be quite useful. Apart from interest in the atypical situations, studies of this type would be useful to further explore the mechanisms responsible for the sequence of events observed in the typical scenario and, in particular, to determine if the remote SST responses somehow feeds back to the Pacific.

The discussions in this paper have emphasized the associations in which the Pacific activity leads both the Indian and North Atlantic regions. However, since the Indian and North Atlantic are also highly correlated with each other, this may be due in part to associations between the two areas, which do not involve the Pacific. In order to briefly address this issue the *partial* correlation has been computed between IND and NATL, removing the effect of their correlations with CPAC. While the simple correlation (average reported in Table 1) between IND and NATL is 0.45, their partial correlation with respect to CPAC is 0.37. While this does suggest some association exclusive of the Pacific, more effort (along the lines described above) would be needed to make a convincing case to support this.

Acknowledgments. The COADS data were kindly provided by Bram Oort and the GOSTA data by Tom Delworth. The constructive comments provided by Gabriel Lau and Tom Knutson in reviewing this manuscript are appreciated. Gabriel Lau generously shared cross-spectral analyses from an earlier study. An anonymous reviewer also provided useful comments. Some assistance in figure preparation was provided by Cathy Raphael and Jeff Varanyak.

REFERENCES

Barnett, T., 1983: Interaction of the monsoon and Pacific trade wind system at interannual time scales. Part I: The equatorial zone. *Mon. Wea. Rev.,* 111, 756–773.

Bottomley, M., C. Folland, J. Hsiung, R. Newell, and D. Parker, 1990: *Global Ocean Surface Temperature Atlas (GOSTA).* Her Majesty's Stationery Office, 337 pp.

Covey, D., and S. Hastenrath, 1978: The Pacific El Niño phenomenon and the Atlantic circulation. *Mon. Wea. Rev.,* 106, 1280–1287.

Duchon, C., 1979: Lanczos filtering in one and two dimensions. *J. Appl. Meteor.,* 18, 1016–1022.

Graham, N., T. Barnett, R. Wilde, M. Ponater, and S. Schubert, 1994: On the roles of tropical and midlatitude SSTs in forcing interannual to interdecadal variability in the winter Northern Hemisphere circulation. *J. Climate,* 7, 1416–1442.

Gu, D., and S. Philander, 1995: Secular changes of annual and interannual variability in the Tropics during the past century. *J. Climate,* 8, 864–876.

Horel, J., 1984: Complex principal component analysis: Theory and examples. *J. Climate Appl. Meteor.,* 23, 1660–1673.

Hsiung, J., and R. Newell, 1983: The principal nonseasonal modes of variation of global sea surface temperature. *J. Phys. Oceanogr.,* 13, 1957–1967.

Kawamura, R., 1994: A rotated EOF analysis of global sea surface temperature variability with interannual and interdecadal scales. *J. Phys. Oceanogr.,* 24, 707–715.

Latif, M., and T. Barnett, 1995: Interactions of the tropical oceans. *J. Climate,* 8, 952–964.

Lau, N-C., and M. Nath, 1994: A modeling study of the relative roles of tropical and extratropical SST anomalies in the variability of the global atmosphere–ocean system. *J. Climate,* 7, 1184–1207.

Pan, Y-H., and A. Oort, 1990: Correlation analyses between sea surface temperature anomalies in the eastern equatorial Pacific and the world ocean. *Climate Dyn.,* 4, 191–205.

Philander, S., 1990: *El Niño, La Niña, and the Southern Oscillation.* Academic Press, 293 pp.

Rasmusson, E., and T. Carpenter, 1982: Variations in tropical sea surface temperature and surface wind fields associated with the Southern Oscillation/El Niño. *Mon. Wea. Rev.,* 110, 354–384.

——, X. Wang, and C. Ropelewski, 1990: The biennial component of ENSO variability. *J. Mar. Syst.,* 110, 71–96.

Tourre, Y., and W. White, 1995: ENSO signals in global upper-ocean temperature. *J. Phys. Oceanogr.,* 25, 1317–1332.

Wolter, K., 1987: The Southern Oscillation in surface circulation and climate over the tropical Atlantic, eastern Pacific, and Indian Oceans as captured by cluster analysis. *J. Climate Appl. Meteor.,* 26, 540–558.

Woodruff, S., R. Slutz, R. Jenne, and P. Steurer, 1987: A Comprehensive Ocean–Atmosphere Data Set. *Bull. Amer. Meteor. Soc.,* 68, 1239–1250.

Wright, P., 1989: Homogenized long-period southern oscillation indices. *Int. J. Climatol.,* 9, 33–54.

Zar, J., 1974: *Biostatistical Analysis.* Prentice-Hall, 620 pp.

Zebiak, S., 1993: Air–sea interactions in the equatorial Atlantic region. *J. Climate,* 6, 1567–1586.